Transactions of the TSME (2017) Vol. 5, No. 2, 82-93
Journal of Research and Applications in Mechanical Engineering

ISSN 2229-2152 print
DOI: 10.14456/jrame.2017.8

Research Article

EFFECT OF INSTALLED PHOTOVOLTAIC ARRAY CAPACITY ON THE PERFORMANCE OF SURFACE PUMPING SYSTEMS

M. Rungsiyopas[1,*]
C. Chuenwattanapraniti[2]
[1] *Department of Mechanical Engineering, Faculty of Engineering, Burapha University, 169 Longhaad Bangsaen Road, Saensook, Mueang, Chonburi, 20131, Thailand*
[2] *Department of Electrical Engineering, Faculty of Engineering, Burapha University, 169 Longhaad Bangsaen Road, Saensook, Mueang, Chonburi, 20131, Thailand*

ABSTRACT:
This research aims to study the effect of installed photovoltaic (PV) capacity on performance of surface pump powered by photovoltaic array under several heads. The PV pumping system test rig was developed in laboratory and the data collected from the experiments were used for water flow rate prediction. In the experiments, for a particular head, numbers of PV module are varied. The daily water flow rate for each system configuration is also estimated and compared with the others. Finally, the subsystem efficiencies were calculated in order to indicate the effect of installed PV generation capacity. This performance comparison allows the system designers to optimize the PV array sizes to achieve high system efficient and cover their daily water demand.

Keywords: *Photovoltaic, PV pumping system, Surface pump, Pump performance*

1. INTRODUCTION

In many recent years, due to the rapid growth of PV market, the price of PV panel has been decreased rapidly [1].Therefore the solar pumping system is an attractive choice to replace diesel engine-driven pump especially for the livestock and crop irrigation in remote areas. Additionally, it assures the independence from diesel prices and low maintenance cost result in the shortening of payback period.

Solar water pumps may be divided into three applications: village water supply, livestock and agricultural watering, and irrigation. Surface solar pump draws water from shallow wells for agricultural water supply in which water head is less than 10 m. For village water supply system, it is necessary to ensure the continuous of water supply by storing in tower tank which require the high pump pressure to overcome the high head loss. Reciprocating pumps particularly use to meet the pressure requirement, whereas centrifugal pumps provide the capacity scale [2].

Some researchers studied the simple PV pumping systems in which PV array directly coupled to a DC motor driven pump. A. Djoudi Gherbi, et al. [3] developed the PV motor-pump model for system performance analysis. However, due to a directly connected motor to PV array, the maximum possible PV power could not be achieved. To improve the system performance, a DC-DC converter interfaced between PV array and motor-pump should be employed. Ghoneim [4] developed a computer program to determine the performance of PV pumping system driven by DC motor. Protogeropoulos and Pearce proposed the sizing charts for such system based on field testing data [5].

* Corresponding author: M. Rungsiyopas
E-mail address: montana@eng.buu.ac.th

However, most of commercialized centrifugal pumps sized from ½ HP are usually driven by AC motors (induction type) which provide more reliable, cost competitive and lower maintenance cost than DC motors [6 – 8]. In the case of AC motor, the solar pump inverter interfaced between PV array and motor are required to convert DC to AC electricity and also tracking the maximum power point of array. In several years, many control strategies concerned in AC pumping system have been proposed to enhance the pumping performance [9 – 11].

Since Thailand is an agricultural country, therefore this research focuses on the centrifugal pump to serve the flow capacity demand. Matching between the PV generated capacity and pumping head is an important issue because it affects to the system performance and total investment cost. In addition, poor design of the system leads to low efficiency, high cost and mismatch of components. Most of system designer select the number of installed PV module by considering the sufficient DC voltage to supply at the inverter DC terminal. For example, to drive the 220 V AC motor, it is necessary to supply 310 V array voltage which may be underperform when driving light load conditions.

This paper presents the pumping performance comparison among three different PV array configurations which provide three difference operating voltages. The experiments are also carried out with three pumping head under real solar radiation. The performance investigation is derived from the empirical models based on the test results collected from pumping test facility at Burapha University. This method performed more realistic than mathematical model because in real conditions the pump, motor, and inverter characteristic may alter from their specifications provided by vendors.

2. METHODOLOGY

2.1 System configuration and data collection

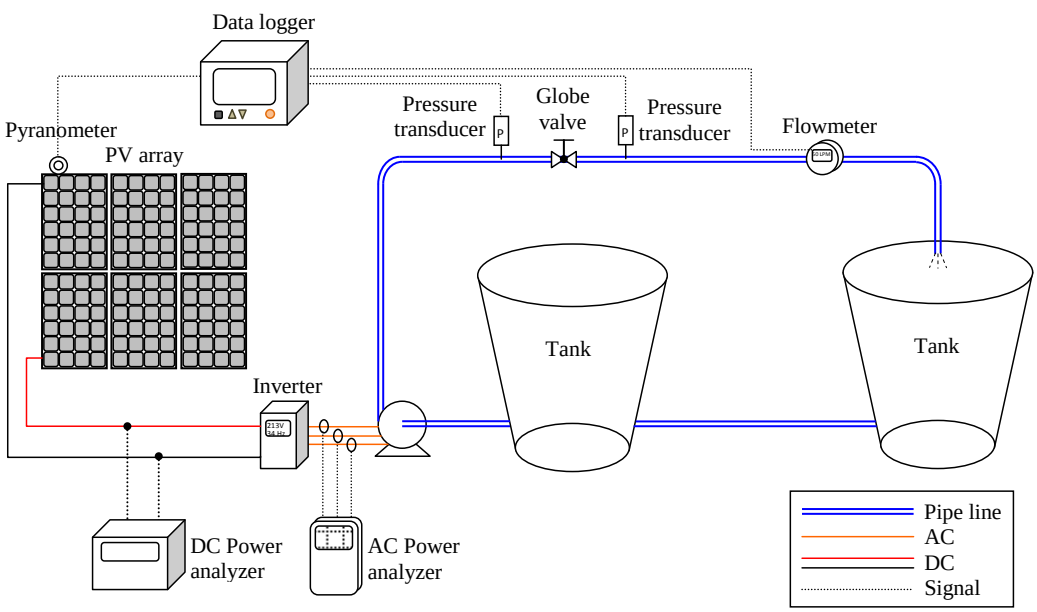

Fig. 1. The diagram for PV water pumping system and data acquisitions.

The PV water pumping system consists of polycrystalline silicon type of 290 W photovoltaic modules, centrifugal pump of 1.5 hp driven by three phase AC motor, DC to AC inverter, control valve, and two tanks of 2500 L. The proposed PV modules were mounted on supporting with tilt angle equal to 13o and facing to south direction. The 5, 6, and 8 modules of polycrystalline silicon were connected in series depend upon experimental setting up. The characteristics of the PV module and the specification of centrifugal pump are given by Table 1 and Table 2. A Yokogawa magnetic flow meter model AXF040G, two Trafag pressure transducers type 8472.26.5717, a Kipp and Zonen SP-Lite pyranometer, and the thermocouple type K were connected to Yokogawa data logger model GP10 in order to gather volume flow rate, pressure, solar irradiance, as well as ambient and water temperature. A Yokogawa

power analyzer model WT310 was used to measure PV voltage, current, and power on DC side of inverter while a Metrel power analyzer model MI-2892 was used to measure voltage, current, and power factor at the motor-pump terminal. The diagram for PV water pumping system configuration including all data acquisitions is shown in Fig. 1 and the experimental equipment of water pumping system are presented Fig. 2. The water was pumped from the first tank to the second tank and then it drained back to the first one.

(a) PV array setup on rooftop of building.

(b) Water pumping test.

(c) Measuring equipment

Fig. 2. The water pumping system and measuring equipment (a) PV array setup on rooftop of building, (b) Water pumping test, and (c) Measuring equipment.

Table 1: Characteristics of the photovoltaic module

Photovoltaic type	Polycrystalline silicon
Model	SUNTECH STP290-24Ve
Maximum power	290 W_p
Module efficiency	14.9%
Voltage at mpp, V_{mpp}	35.6 V
Current at mpp, I_{mpp}	8.15 A
Open circuit voltage, V_{oc}	45.0 V
Short circuit current, I_{sc}	8.42 A
Dimensions	1956mm × 992mm × 40mm

Table 2: Specification of centrifugal pump

Pump type	Single impeller centrifugal
Model	Venz VC150
Maximum/minimum head	28 m/5 m
Design flow rate	10 – 450 l/min
Maximum pressure	6 bars
Input/output port	2-inch/2-inch
Materials	Cast iron body, Brass impeller
Motor type	Three–phase induction motor
Rated voltage	220 – 240 V (delta)
Rated current	4.4 A
Rated power	1.5 HP/1.1 kW
Frequency	50 Hz

2.2 Total head loss calculation

The total head, H at any operation time of the standalone PV water pumping system can be represented as follows:

$$H = H_s + H_{L,f} + H_{L,e} \tag{1}$$

where H_s is the static head and equal to the difference height between the surface of water and the discharge point. $H_{L,f}$ is the major head loss or the dynamic head due to friction loss in pipeline can be calculated based on the Darcy-Weisbach formula:

$$H_{L,f} = f\frac{L}{D}\frac{v^2}{2g} \tag{2}$$

where f is the friction factor depends on Reynolds number and the type of flow in pipe (Laminar or turbulent)
L is the length of the pipeline (5 m),
D is the inside diameter of the pipeline (0.0508 m),
g is the acceleration due to gravity,
v is the average velocity of the water (m/s) which is related to the water flow rate and the cross-sectional area of the pipe line as below
$H_{L,e}$ is the minor head loss due to the fitting components can be calculated from Eq.(3).

$$H_{L,e} = K\frac{v^2}{2g} \tag{3}$$

where K is the fitting loss coefficient depending on the type of accessories (valves, tee junction, elbows, reducing pipe,…).
This method of calculation (Eqs.1 – 3) is used for prelimary design in case of steady flow rate. In solar powered system which generated unsteady flow and head, it is necessary to simulate system head so globe valve is then setup for this purpose.

2.3 Inverter setting

For a given irradiance and cell temperature, the output power of PV panel depends on the operating point on its I-V curve. The maximum power could be extracted from PV module if PV panel operates at the optimal point. This point is known as maximum power point (MPP) which normally locates at the knee point of I-V curve.

In PV pumping system driven by induction motor, the inverter interfaced between PV array and motor is used to convert the DC voltage to AC voltage. To track the maximum power point, the inverter varies its output frequency until the maximum power point is reached. In addition, the inverter output voltage is controlled to follow the fixed V/F ratio in order to maintain maximum torque. Therefore, in case of 5 and 6-Module array, inverter will then limit its maximum output frequency at low value due to its low DC input voltage. In most conditions, the maximum power operating point may not be achieved. For a maximum power point tracking purpose, the "Boost Factor" should be introduced in both cases since it will enable the inverter output frequency to increase beyond the actual frequency limitation. The boost factor will take place only when the DC voltage is higher than the predefined "Boost Voltage".

In the experiments, the "Boost Factor" for 8, 6, 5-module array were set at 1.0 (disable), 1.1 and 1.2 respectively while the "Boost Voltage" were set corresponding to the nominal maximum power point voltage (V_{mpp}) of PV array.

2.4 Volume flow rate prediction

In PV pumping system, the water flow rate mainly depends on the irradiance, head and number of installed PV module. In order to predict the instantaneous flow rate at any operating condition, the flow rate as a function of head and irradiance was written as follows:

$$Q(H,G) = \left(a_1G^3 + a_2G^2 + a_3G + a_4\right)H^2 + \left(a_5G^3 + a_6G^2 + a_7G + a_8\right)H + \left(a_9G^3 + a_{10}G^2 + a_{11}G + a_{12}\right) \tag{4}$$

The coefficients a_1 to a_{12} in Eq. (4) were derived from the flow vs head data at specific irradiance which collected from the experiments. By polynomial regression, the coefficients of polynomial function can be obtained. Table 3 presents the coefficients for each array configurations.

Table 3: Coefficients of correlation for water flow rate prediction

Coefficient	8 Modules	6 Modules	5 Modules	Coefficient	8 Modules	6 Modules	5 Modules
a_1	-3.50×10^{-9}	7.80×10^{-10}	1.01×10^{-7}	a_7	0.195873	0.050983	-0.294462
a_2	6.81×10^{-6}	-1.69×10^{-5}	-2.00×10^{-4}	a_8	-50.000000	-15.000000	46.428401
a_3	-4.28×10^{-3}	-1.19×10^{-2}	0.122770	a_9	0	2.14×10^{-7}	5.39×10^{-7}
a_4	0.350000	-4.000000	-24.743130	a_{10}	-2.33×10^{-4}	-5.85×10^{-4}	-1.16×10^{-3}
a_5	1.33×10^{-7}	3.24×10^{-8}	-2.64×10^{-7}	a_{11}	0.399579	0.506681	0.817343
a_6	-2.81×10^{-4}	-7.09×10^{-5}	5.10×10^{-4}	a_{12}	141.389082	105.000000	22.395121

2.5 Efficiency calculation

For the estimation of PV array production under various operating conditions, modeling of a single PV cell is required. The one diode model as illustrated in Fig. 3 is employed in this research to determine the theoretically maximum array output power at any irradiance. To simplify the model, the shunt resistance (R_{sh}) is neglected so that the current-voltage $(I-V)$ characteristic of PV cell is given by:

$$I = I_{sc} - I_0\left(e^{\left(\frac{IR_s+V}{V_T}\right)}-1\right) \tag{5}$$

where R_s represent series resistance of PV cell, V_T is thermal voltage which is 26 mV, I_{sc} is short circuit current for a given irradiance and I_0 is reverse saturation current.

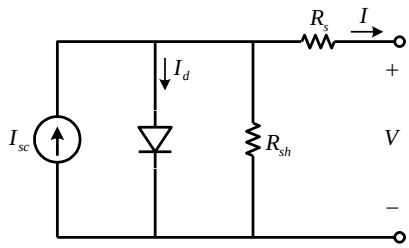

Fig. 3. Generalized model of a solar cell.

Once the electrical characteristics of PV module at standard condition have known and assuming a constant cell temperature at 25˚C, the current at maximum power point at any irradiance (G) which is directly related to irradiance can be calculated:

$$I_{mpp} = \frac{G}{1000} I_{mpp,STC} \tag{6}$$

where I_{mpp} and $I_{mpp,STC}$ are current at maximum power point for a given irradiance and standard test condition (STC) respectively.

Rewrite equation (5) for maximum power point operating condition:

$$I_{mpp} = I_{sc} - I_0\left(e^{\left(\frac{I_{mpp}R_s+V_{mpp}}{V_T}\right)}-1\right) \tag{7}$$

Based on the knowledge of $I_{mpp}, I_{sc}, I_{sc,STC}$ and $V_{oc,STC}$, the voltage at maximum power point (V_{mpp}) can be calculated as follows:

$$V_{mpp} = V_T \ln\left[1+\frac{I_{sc}-I_{mpp}}{I_{sc,STC}}\left(e^{\frac{V_{oc,STC}}{V_T}}-1\right)\right] - I_{mpp}R_s \tag{8}$$

The theoretically maximum power of a PV module (P_{mpp}) can be determined by

$$P_{mpp} = N\left(V_{mpp}I_{mpp}\right) \text{ per module} \tag{9}$$

where N is the number of cells in the module

The instantaneous water flow rate (Q) is integrated over time to determine the daily water delivery and to calculate the hydraulic energy (E_{hyd}) whereas the maximum power (P_{mpp}) is integrated over time to find the total PV energy using the following relations:

$$E_{hyd} = \rho g H \int_{1\text{day}} Q\,dt \tag{10}$$

$$E_{PV} = \int_{1day} P_{mpp}\,dt \tag{11}$$

Then, the percentage use of PV energy is calculated by,

$$\%\ \text{used PV energy} = \frac{E_{hyd}}{E_{PV}} \times 100 \tag{12}$$

The hydraulic power (P_{hyd}) for a specific head (H) is determined using water flow rate (Q). The system input power is derived from incident solar radiation (G) on the panel area (A), thus the instantaneous system efficiency becomes

$$\eta_{sys} = \frac{P_{hyd}}{GA} = \frac{\rho g H Q}{GA} \tag{13}$$

The inverter $\left(\eta_{inv}\right)$ and motor-pump $\left(\eta_{motor-pump}\right)$ efficiencies are included to establish the sub–system efficiency as following

$$\eta_{sub-sys} = \eta_{inv}\eta_{motor-pump} = \frac{P_{hyd}}{P_{PV}} \tag{14}$$

where P_{PV} is measured PV power.

3. Results and Discussion

Based on Eq. (1), the prediction of instantaneous flow rate during the daylight can be calculated. Fig. 4 shows the example of predicted flow rate obtained from the model which is simulated with real irradiance profile in a day providing 5 kWh/m^2 or 5 PSH solar radiations [12, 13]. Fig. 4(a) shows the results for 10 m head. It can be noted that the system supplied from PV array consisted of 5 modules does not have enough power to overcome the hydraulic load therefore the flow rate is zero all day. As the number of module was increased to be 6 modules, the pump starts to delivery water around 9AM which correspond to 400 W/m^2 of irradiance. However, for this PV configuration the water flow rate was limited around 100 l/min throughout the day due to the limitation of V/F control. At this condition the PV array did not operate at MPP. Increasing to the 8-module array provides higher water flow rate than 6-module array as expected.

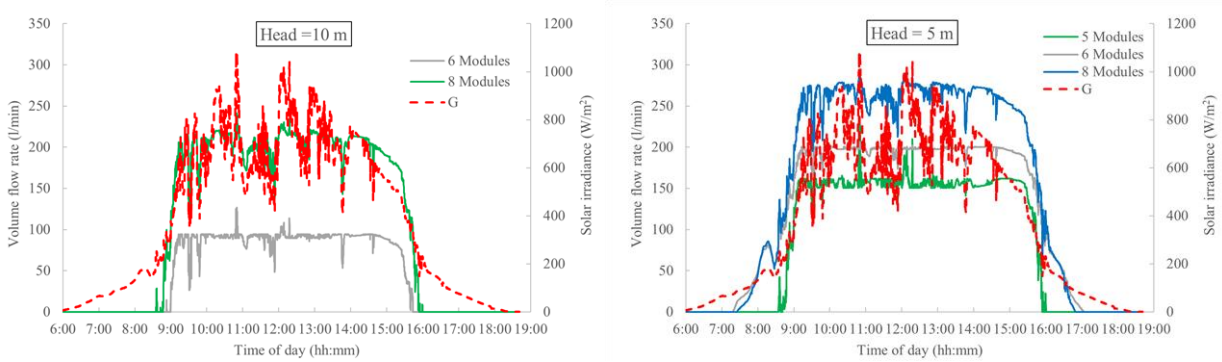

(a) 10 m

(b) 5 m

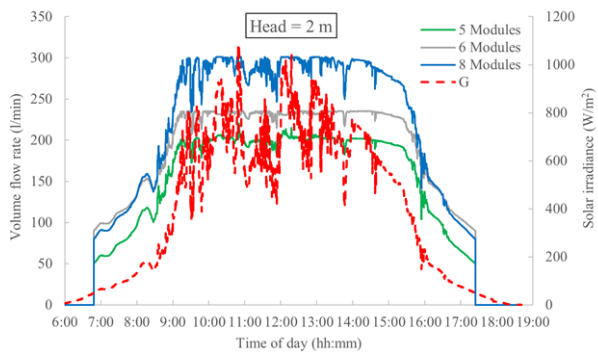

(c) 2 m

Fig. 4. Prediction of instantaneous volume flow rate during 5–PSH day for three different total heads (a) 10 m, (b) 5 m, and (c) 2 m.

It can be observed from Fig.4 (b) that the 6 and 8-module array start to run at the same time while the 5-module array starts 1 hour later. For 2 m head (Fig.4(c)), all PV configurations start to run at the same time in the early morning. In conclusion, water head effects to the cut–in and cut–off time. The pumping period is shorter for higher head.

The total daily water delivery for each configuration is summarized in Table 4. To compare the worthiness among 3 array configurations, the daily water delivery per-module is also calculated. For the high head, the 8-module array shows the best performance among them. When head was decreased to be 5 m, the 6 and 8-module array exhibit better performance than 5-module array. For 2 m head, it can be obviously seen that the 5 and 6-module array provide better water delivery per-module.

Table 4: Daily flow rate for different system configurations

Head	8 Modules		6 Modules		5 Modules	
	Daily flow rate (m^3)	Daily flow rate per module (m^3/module)	Daily flow rate (m^3)	Daily flow rate per module (m^3/module)	Daily flow rate (m^3)	Daily flow rate per module (m^3/module)
10 m	81.27	**10.16**	35.07	5.85	0	0
5 m	116.12	14.52	89.98	**15**	64.66	12.93
2 m	145.92	18.24	123.82	**20.63**	101.98	20.40

The system efficiency was then investigated in order to explain the variation of daily flow rate per module with the array configuration. It is clearly seen in Fig.5 (a) that for 8 modules the highest system efficiency is at 10 m head. Compared the result with 6 and 5 modules in Fig.5 (b) and (c), the system efficiency and the total water delivery per module in this case is maximum. The daily water flow rate is increased when the pumping head is decreased but

the optimum number of modules for 5 m and 2 m pumping head are 6 modules since it provides maximum system efficiency and maximum the daily flow rate per module.

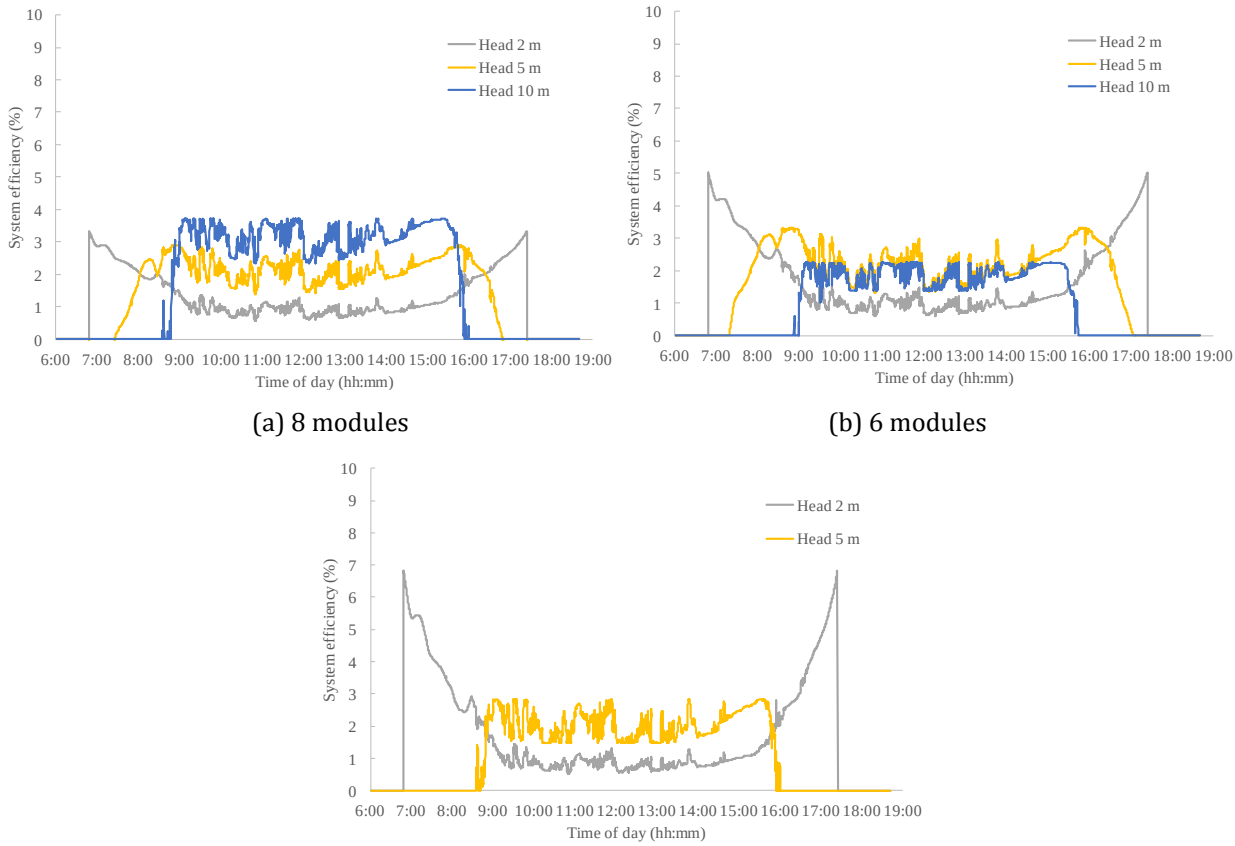

(a) 8 modules

(b) 6 modules

(c) 5 modules

Fig. 5. The variation of system efficiency with time of day (5 PSH) for three different PV arrays (a) 5 PVs, (b) 6 PVs, and (c) 8 PVs.

Since the solar irradiance is generally variable, the instantaneous efficiency stated in Fig.5 cannot well described the utilization of solar energy which converted to hydraulic form. For example, in Fig.5 (c) at 7:00 – 9:00 am the system efficiency for 2 m head is higher than 5 m head but it is just only short period. It is therefore desirable to describe the performance of PV pumping system by total system energy efficiency.

The percentage of used PV energy is presented instead of total system energy efficiency since unavailable energy due to loss in conversion of solar to electrical energy by PV array is practically uncontrolled. Fig. 6 shows that for 2 and 5 m head, 6–module array exhibits the highest percentage of used PV energy whereas for 10 m head, 8–module array contributes the highest.

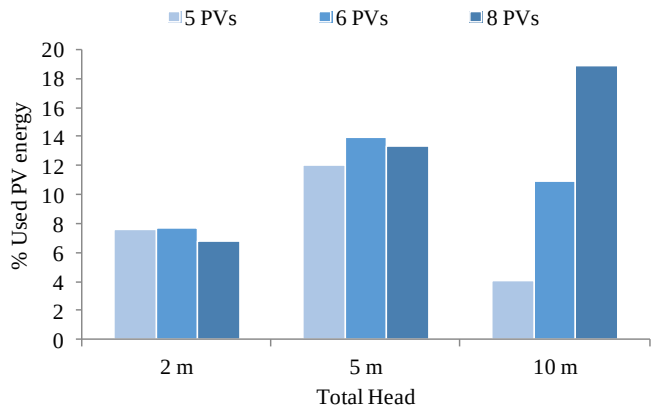

Fig.6. Percentage of used PV energy at different heads and PV arrays.

To clearly discussion about the effect of PV array size on the system performance, sets of subsystem efficiency are illustrated in Fig.7. Due to the advanced technologies in the commercialized solar pump inverters, their efficiency can be generally kept constant around 90-95% whether it operates at full or light load condition. Therefore the motor-pump efficiency is a major factor affecting to the subsystem efficiency. From Fig. 7(a) and (b), it can be concluded that oversized PV array in low and medium head application results in low subsystem efficiency since the pump is operated far away from its best efficiency point (BEP). In contrast, for high head condition, the number of installed PV module should be increased in order to achieve the better operating point as shown in Fig.7 (c).

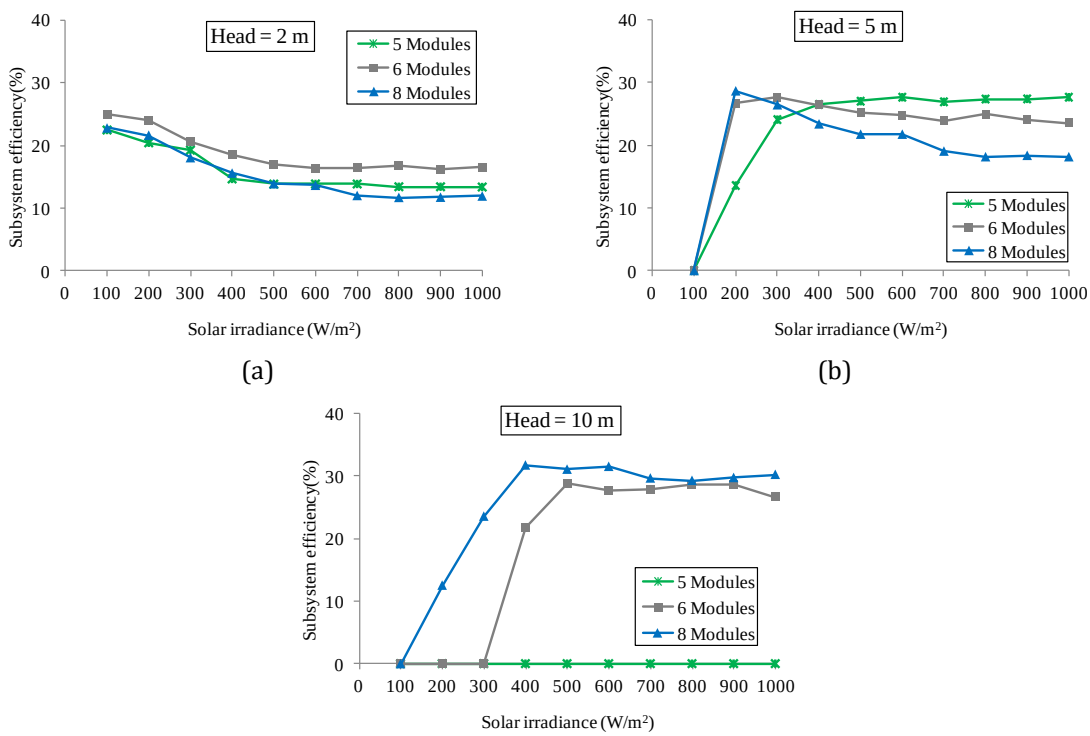

Fig.7. The variation of sub-system efficiency with solar irradiance at different heads and PV arrays (a) 2 m head, (b) 5 m head, and (c) 10 m head.

4. CONCLUSION

The effect of installed PV capacity on the pumping performance has been proposed. The PV pumping test rig has been established in laboratory. The 1.1 kW motor-pump set was selected in our study since it can serve the daily water requirement for small-scale water pumping system. The collected data from the experimental set are used for system modeling and then system performance assessment. It can be concluded that for high head (10m) application, it should be installed the sufficient number of module in order to achieve the satisfactory system efficiency and gain maximum use of PV energy. In contrast, for head ranged between 2–5 m, oversized PV generation lead to low efficiency of overall efficiency. For these cases, it is obvious from the daily flow rate per module as well as the percent used PV energy that 6 PV modules has the best system performance which makes it more suitable and economical. The comparison of daily water delivery for each system configuration is also summarized. Since the investment cost of PV pumping system and payback period strongly depend on the price of PV panel, the system designer should well aware of the installed PV capacity to match their requirements.

ACKNOWLEDGEMENTS

The authors are grateful to The Coordinating Center for Thai Government Science and Technology Scholarship Students (CSTS), National Science and Technology Development Agency (NSTDA), Thailand for funding our research project under contract no. FDA-CO-2558-967-TH and project no. SCH-NR2015-251.

NOMENCLATURE

A	panel area, m^2
D	inside diameter of the pipeline, m
E_{hyd}	hydraulic energy, Wh
E_{PV}	PV energy, Wh
f	friction factor
g	acceleration due to gravity, m/s^2
G	solar radiation, W/m^2
H	total head, m
$H_{L,e}$	head loss due to fitting components, m
$H_{L,f}$	dynamic head due to friction loss, m
H_S	static head, m
I	PV cell output current, A
I_0	PV cell reverse saturation current, A
I_{mpp}	PV module's maximum power point current, A
$I_{mpp,STC}$	PV module's maximum power point current for standard test condition, A
I_{sc}	PV module's short circuit current, A
$I_{sc,STC}$	PV module's short circuit current for standard test condition, A
K	fitting loss coefficient
L	length of the pipeline, m
N	number of cell in the module
P_{hyd}	hydraulic power, W
P_{mpp}	PV module's maximum power, W
Q	volume flow rate, l/min
R_s	PV cell series resistance, Ω
R_{sh}	PV cell shunt resistance, Ω
t	time, h
v	average velocity of the water, m/s

V PV cell output voltage, V

V_{mpp} PV module's maximum power point voltage, V

V_{oc} PV module's open circuit voltage, V

$V_{oc,STC}$ PV module's open circuit voltage for standard test condition, A

V_T thermal voltage, V

η_{inv} inverter efficiency

$\eta_{motor-pump}$ motor-pump efficiency

$\eta_{sub-sys}$ sub-system efficiency

η_{sys} system efficiency

ρ water density, kg/m^3

REFERENCES

[1] Fu, R., Feldman, D., Margolis, R., Woodhouse, M. and Ardani, K. U.S. Solar Photovoltaic System Cost Benchmark Q1, 2017, National Renewable Energy Laboratory, Colorado.

[2] Igor, J. Karassik, Joseph, P. Messina, Paul Cooper and Charles, C. Heald, Pump Handbook, Fourth edition, 2008, McGraw Hill Companies, New york

[3] Djoudi Gherbi, A., Hadj Arab, A. and Salhi, H. Improvement and validation of PV motor-pump model for PV pumping system performance analysis. Solar Energy, Vol. 144, 2017, pp. 310-320.

[4] Ghoneim, A.A. Design optimization of photovoltaic powered water pumping systems. Energy Conversion and Management, Vol. 47, 2006, pp. 1449-1463.

[5] Protogeropoulos, C. and Pearce, S. Laboratory evaluation and system sizing charts for a second generation direct PV-powered, low cost submersible solar pump. Solar Energy, Vol. 68(5), 2000, pp. 453-474.

[6] Mona, N. Eskander and Aziza, M. Zaki, A maximum efficiency photovoltaic-induction motor pump system. Renewable Energy, Vol. 10(1), 1997, pp. 53-60.

[7] Zaki, A. and Eskander, M. Matching of photovoltaic motor–pump systems for maximum efficiency operation. Renewable Energy, Vol. 7(3), 1996, pp. 279-288.

[8] Betka, A. and Moussi, A. Performance optimization of a photovoltaic induction motor pumping system. Renewable Energy, Vol. 29, 2004, pp. 2167-2181.

[9] Muljadi, E. PV Water Pumping with a Peak-Power Tracker Using a Simple Six-Step Square-Wave Inverter. IEEE Transactions on industry applications, Vol. 33(3), May/June, 1997, pp. 714-721.

[10] Miladi, M., Ben Abdelghani-Bennani, A., Slama-Belkhodja, I. and M'Saad, H. Improved low cost induction motor control for stand alone solar pumping. International Conference on Electrical Sciences and Technologies in Maghreb (CISTEM), 2014, pp. 1-8.

[11] Aashoor, F.A.O. and Robinson F.V.P. Maximum power point tracking of photovoltaic water pumping system using fuzzy logic controller. Power Engineering Conference (UPEC), 2013, 48th International Universities.

[12] Department of Alternative Energy Development and Efficiency, Ministry of Energy. The solar radiation map. Bangkok, 2009.

[13] Janjai, S., Laksanaboonsong, J., Nunez, M. and Thongsathitya, A. Development of a method for generating operational solar radiation maps from satellite data for a tropical environment. Solar Energy, Vol. 78, 2005, pp. 739-751.